Gynecologic Oncology 165 (2022) 114–120

Contents lists available at ScienceDirect

Gynecologic Oncology

journal homepage: www.elsevier.com/locate/ygyno

Signal transduction pathway activity in high-grade serous carcinoma, its precursors and Fallopian tube epithelium

Phyllis van der Ploeg [a,b,*], Aniek Uittenboogaard [a,1], Steven L. Bosch [c], Paul J. van Diest [d], Yvonne J.W. Wesseling-Rozendaal [e], Anja van de Stolpe [e], Sandrina Lambrechts [f], Ruud L.M. Bekkers [a,b], Jurgen M.J. Piek [a]

[a] Department of Obstetrics and Gynecology, Catharina Cancer Institute, Catharina Hospital, Eindhoven, the Netherlands
[b] GROW School for Oncology and Developmental Biology, Maastricht University, Maastricht, the Netherlands
[c] Laboratory for Pathology and Medical Microbiology (Stichting PAMM), Eindhoven, the Netherlands
[d] Department of Pathology, University Medical Center Utrecht, Utrecht, the Netherlands
[e] Molecular Pathway Diagnostics, Philips Research, Eindhoven, the Netherlands
[f] Department of Obstetrics and Gynecology, Maastricht University Medical Center+, Maastricht, the Netherlands

HIGHLIGHTS

- Aberrant PI3K, HH and ER pathway activity might be putative early drivers of neoplastic transformation of FTE into STIC.
- STIC and concurrent HGSC showed loss of FOXO3a protein expression in comparison to normal FTE.
- Loss of AR and Wnt pathway activity are more likely to be contributors of HGSC progression.

ARTICLE INFO

Article history:
Received 24 October 2021
Received in revised form 14 January 2022
Accepted 24 January 2022
Available online 2 February 2022

Keywords:
Serous tubal intraepithelial carcinoma
Serous carcinogenesis
Molecular biology
PI3K-FOXO signaling

ABSTRACT

Objective. To determine the activity of key signal transduction pathways in serous tubal intraepithelial carcinoma (STIC) and concurrent high-grade serous carcinoma (HGSC) and compare this to pathway activity in normal Fallopian tube epithelium (FTE).

Methods. We assessed mRNA expression levels of pathway-specific target genes with RT-qPCR in STIC and concurrent HGSC ($n = 8$) and normal FTE ($n = 8$). Subsequently, signal transduction pathway assays were used to assess functional activity of the androgen (AR) and estrogen receptor (ER), phosphoinositide-3-kinase (PI3K), Hedgehog (HH), transforming growth factor beta (TGF-β) and canonical wingless-type MMTV integration site (Wnt) pathways.

Results. There were no statistically significant differences in pathway activity between STIC and HGSC, but STIC and HGSC demonstrated significantly lower ER and higher PI3K and HH pathway activity in comparison to normal FTE, suggesting these pathways as putative early drivers. In addition, we determined FOXO3a protein expression by immunohistochemistry and found loss of FOXO3a protein expression in STIC and HGSC compared to normal FTE. This observation confirmed that activation of PI3K signaling by loss of FOXO is an early hallmark of serous carcinogenesis. Furthermore, HGSC demonstrated significant loss of AR and Wnt pathway activity in relation to FTE, suggesting these pathways contribute to disease progression.

Conclusion. Our observations, together with the previously described associations between p53 signaling and both PI3K and HH pathway activity, provide evidence that increased PI3K and HH pathway activity and loss of ER pathway activity may be underlying events contributing to neoplastic transformation of FTE into STIC.

* Corresponding author at: Department of Obstetrics and Gynecology, Catharina Hospital, Michelangelolaan 2, 5623 EJ Eindhoven, the Netherlands.
E-mail address: phyllis.vd.ploeg@catharinaziekenhuis.nl (P. van der Ploeg).
[1] Present address: Department of Pediatric Oncology, Emma's Children Hospital, Amsterdam UMC, Vrije Universiteit Amsterdam, the Netherlands.

https://doi.org/10.1016/j.ygyno.2022.01.027

List of abbreviations

AR	Androgen receptor
BMI	Body mass index
ER	Estrogen receptor
FFPE	Formalin-fixed paraffin-embedded
FOXO	Forkhead box protein o
FTE	Fallopian tube epithelium
H&E	Hematoxylin and eosin
HGSC	High-grade serous carcinoma
HH	Hedgehog
IQR	Interquartile range
PI3K	Phosphoinositide-3-kinase
RT-qPCR	Real-time quantitative reverse transcription polymerase chain reaction
STIC	Serous tubal intraepithelial carcinoma
STMN1	Stathmin 1
STPs	Signal transduction pathways
TGF-β	Transforming growth factor-beta
Wnt	Canonical wingless-type MMTV integration site

1. Introduction

Nonuterine high-grade serous carcinoma (HGSC) refers to ovarian, Fallopian tube and primary peritoneal cancers [1]. HGSC typically present at an advanced stage, requiring treatment consisting of platinum-based chemotherapy and debulking surgery. Unfortunately, current treatment is insufficient to acquire long-term survival, as in more than 50% of the patients relapse of disease occurs within two years and becomes platinum-resistant [2,3]. Therefore, there is an urgent need to elucidate early cellular processes leading to HGSC in order to identify new leads for treatment options.

Traditionally, the ovarian surface epithelium was proposed as the cell of origin of HGSC [4]. Two decades ago, another hypothesis evolved as preneoplastic changes were observed in the epithelium of the fimbriae of prophylactically removed Fallopian tubes of women with a hereditary high risk to develop HGSC, but not in the ovarian surface epithelium [5,6]. These non-invasive dysplastic precursor lesions, later named serous tubal intraepithelial carcinoma (STIC), were also observed in Fallopian tubes of women with non-hereditary HGSC [7]. Proof of a clonal relationship between STIC and HGSC was given by the observation of identical mutations in the tumor suppressor gene *TP53* in paired cases of STIC and HGSC [8]. Furthermore, transformation of Fallopian tube secretory cells in genetically modified mice resulted in the development of lesions mimicking STIC and HGSC [9]. Additionally, xenografted tumors in mice derived from transformed human tubal stem cells showed similar histological and molecular characteristics as HGSC, suggesting a causal relation [10]. Finally, the tubal hypothesis received additional support from molecular profiling studies as STIC were found to have genetic features closely resembling HGSC [11,12].

Despite accumulating evidence supporting Fallopian tube epithelium (FTE) as the cell of origin of most HGSC, the initial molecular processes underlying the transformation of FTE into STIC and HGSC remain poorly understood. Previously, loss of forkhead box protein O3a (FOXO3a) was suggested to be an early event in STIC [13]. FOXO3a is a tumor suppressive transcription factor of the forkhead family and is negatively regulated by the phosphoinositide-3-kinase (PI3K) growth factor signaling pathway [14]. The association between loss of FOXO3a and poor prognosis further supported the clinical relevance of PI3K-FOXO signaling in HGSC [15,16]. In addition to the PI3K pathway, heterogenous activity of other key signal transduction pathways (STPs) has been observed among HGSC samples, for instance the androgen (AR) and estrogen receptor (ER), Hedgehog (HH), transforming growth factor beta (TGF-β) and canonical wingless-type MMTV integration site (Wnt) pathways [17]. The wide variety in STP activity suggests unique tumor activation patterns [17]. Determining whether these STPs are also activated in STIC could improve our understanding of aberrant STP activity, and subsequently enable the characterization of early events of high-grade serous carcinogenesis.

Therefore, we investigated in this study the activity of the AR, ER, PI3K, HH, TGF-β and Wnt pathways in STIC and concurrent HGSC in relation to the STP activity in morphologically normal FTE. We aim to identify early aberrations in STP activity that may contribute to the processes related to neoplastic transformation of FTE into HGSC.

2. Materials and methods

2.1. Study design and population

We searched the pathology archive of the Catharina Hospital in Eindhoven, The Netherlands for morphologically normal Fallopian tubes obtained from healthy postmenopausal women who had surgery for benign gynecological conditions between 2009 and 2018. Women were excluded in case of a history of gynecological cancer, a known pathogenic germline mutation of the *BRCA1/2* genes or other personal or family hereditary risks of cancer. In addition, we searched for women diagnosed with STIC with concurrent HGSC diagnosis between 2004 and 2020. Medical records were screened for demographic and pathological data including, age at the time of surgery, contraceptive use, menopausal status, BMI, parity, FIGO stage and type of treatment.

The study was approved by the Medical research Ethics Committees United (MEC-U, study number W16.108 and W18.134) and was conducted in accordance with the Code of Conduct of the Federation of Medical Scientific Societies in The Netherlands. Written informed consent was obtained from women with benign diagnosis. The MEC-U waived the need for informed consent of women diagnosed with HGSC as the majority of the women would have succumbed from disease at the time of inclusion due to the aggressive nature of the disease. However, medical records were checked for any signs of objection to the use of residual tissue for research purposes.

2.2. Sample preparation

Archived sections were revised by an expert gynecological pathologist (SLB) to confirm the presence of morphologically normal fimbriae, STIC and HGSC. Representative areas were annotated for analysis. Examples of STIC and HGSC are shown in Fig. S1A-D. HGSC samples with less than 40% tumor cell nuclei were excluded to minimize stromal contamination. Five μm formalin-fixed paraffin-embedded (FFPE) sections were cut from the selected tissue blocks with a microtome (RM2255, Leica Biosystems, Germany) and mounted onto PEM-membrane coated slides (normal FTE and STIC samples) or glass slides (HGSC samples). The last section was hematoxylin and eosin (H&E) stained and evaluated for the presence of the annotated area of interest. For normal FTE and STIC samples, intermediate sections were manually hematoxylin stained for visualization of the selected areas. Subsequently, to eliminate stromal contamination, fimbrial epithelial cells and STIC lesions were isolated by laser capture microdissection (PALM MicroBeam 4, Carl Zeiss B.V., Germany). Intermediate sections with HGSC areas were manually scraped for the collection of tumor cells using the last annotated H&E slide as a reference.

2.3. mRNA extraction, RT-qPCR analysis and signal transduction pathway assays

To evaluate STP activity, mRNA was isolated from the normal FTE, STIC and HGSC samples using the VERSANT® Tissue Preparation Reagents kit (Siemens, Germany). Quantitative activity of the AR, ER, PI3K (indirectly, as it is inversely proportional to FOXO transcription factor activity under the condition of absence of oxidative stress [18]), HH, TGF-β and Wnt pathways and the Ki-67 target gene expression were assessed with the use of commercially available OncoSignal pathway assays (Philips MPDx, The Netherlands) [19]. In brief, expression levels of pathway-specific target genes were measured with real-time quantitative reverse transcription-PCR (RT-qPCR) analysis using the

SuperScript™ III Platinum™ One-Step qRT-PCR kit (Invitrogen, Thermo Fisher Scientific, MA, USA) and commercially available OncoSignal 96-well PCR plates (Philips MPDx, The Netherlands). Sufficient mRNA input for pathway analysis was confirmed by an internal quality control of reference genes consisting of a set of common housekeeping genes. Subsequently, functional STP activity scores were calculated and provided by Philips MPDx (The Netherlands). The general Philips MPDx technology to measure STP activity has been described in detail before [19,20]. In brief, for each STP mRNA levels of target genes of the STP-associated transcription factor are measured, and from these mRNA expression data the STP activity is inferred using Bayesian network models. The models consist of three layers corresponding to (1) the transcription factor complex associated to the STP, (2) the direct target genes of the transcription factor complex and (3) the measured mRNA levels. As a result, the models describe the probabilistic activity of the STP transcription complex using the measured mRNA levels as input. Initially, the models were developed and validated using Affymetrix expression microarray datasets enabling the validation on independent data of various cell and tissue types. Pathway-specific target genes were selected based on elaborate literature study and each pathway model included approximately 25 to 35 target genes. Lists of the selected target genes in the original models of the AR, HH and TGF-β pathways [21], ER and Wnt pathways [19] and PI3K pathway [18] have been described previously. Adaptation of the original models to RT-qPCR models enabled the use of FFPE tissue samples and included the best performing target genes, around 12 target genes per pathway. The RT-qPCR models have since been validated on various cell types, as described previously [20,22,23]. Functional STP activity is expressed on a normalized scale from 0 to 100, where 0 indicates the lowest probability of an active pathway, and inversely, 100 the highest probability of an active pathway.

2.4. Immunohistochemical staining of FOXO3a protein

To validate our PI3K pathway activity data, we determined FOXO3a protein expression by immunohistochemistry in normal FTE, STIC and HGSC samples using a Ventana Benchmark XT Autostainer (Ventana Medical Systems, AZ, USA). Four μm FFPE sections of the identical tissue blocks were cut and deparaffinized. After antigen retrieval and blocking of endogenous peroxidase activity, the sections were incubated with the primary anti-human FOXO3a mouse monoclonal antibody (diluted 1:150, CF809449, ThermoFischer Scientific, USA) for one hour at 36° Celsius. Detection of the primary antibody was achieved after incubation with horseradish peroxidase and visualization with hydrogen peroxidase/3,3′-diaminobenzidine. The sections were counterstained with hematoxylin. Normal pancreas and colon tissue were used as a positive control. FOXO3a stained sections were visually reviewed in a blinded manner by two independent pathologists (SLB and PJvD) without knowledge of each other's assessment and STP assay results. Positively stained tumor cell nuclei were reviewed by a semi-quantitative assessment of staining intensity (negative, weak, moderate or strong) and the percentage of positive tumor cells. Histoscores were calculated by the sum of (1 x % weak) + (2 x % moderate) + (3 x % strong), resulting in scores ranging between 0 and 300. For further analysis we used mean histoscores derived from the assessments of both pathologists.

2.5. Statistical analysis

Clinical characteristics of the women with normal FTE were compared with the characteristics of the women diagnosed with STIC and concurrent HGSC using Wilcoxon rank sum tests for continuous variables with a skewed distribution and presented as median with IQR. Fisher's exact tests were used to compare categorical variables between the groups and presented as frequency and percentages. Differences in STP activity scores and FOXO3a histoscores between groups were tested with Wilcoxon rank sum and Kruskal-Wallis tests. Paired analyses were performed using paired Wilcoxon signed-rank tests. Overall concordance between FOXO3a histoscore assessments of both pathologists was evaluated with the intra-class correlation coefficient using a two-way mixed model. Furthermore, Spearman's rank correlation coefficient was used to determine the correlation between FOXO3a histoscores and PI3K pathway activity. Statistical analysis and data visualization were conducted using R (RStudio, Inc. version 1.1.463).

3. Results

3.1. Study population

We identified 13 postmenopausal women with morphologically normal fimbriae and 12 women with STIC and concurrent HGSC. After laser capture microdissection, we excluded five normal FTE and four paired STIC and HGSC samples due to insufficient mRNA concentrations. For one woman, the concurrent HGSC sample was not suitable for further analysis as it contained less than 40% tumor cell nuclei. Thus, eight normal FTE, eight STIC samples and seven concurrent HGSC samples were available for the analysis of STP activity. Clinicopathological characteristics of the study population are presented in Table 1 and Table S1. Women with STIC and concurrent HGSC had a lower body mass index (BMI) ($P = 0.007$) as compared to women in the normal FTE group. There were no differences between the two groups in age at the time of surgery, menopausal status and parity. Women with paired STIC and HGSC were diagnosed with advanced stage disease (FIGO stage IIIC ($n = 6$) or IV ($n = 2$)). These women had primary debulking surgery followed by adjuvant chemotherapy ($n = 3$) or neo-adjuvant chemotherapy and interval debulking surgery ($n = 5$). Consequently, for the latter group STIC and concurrent HGSC samples were taken after the start of chemotherapy. Women in the normal FTE group had had salpingectomy with or without hysterectomy for the following gynecological conditions; benign adnexal mass ($n = 5$), postmenopausal blood loss ($n = 2$) and uterine descensus ($n = 1$). Pathological revision showed no evidence of dysplasia or malignancy.

3.2. Comparable signaling pathway activity in STIC and HGSC samples

We assessed quantitative activity of the AR, ER, PI3K, HH, TGF-β and Wnt pathways and Ki-67 target gene expression using mRNA measurements of pathway-specific target genes [19]. Overall, we observed no differences in median STP activity between grouped STIC ($n = 8$) and HGSC ($n = 7$) samples (Fig. 1A-G). Subsequent, analysis of paired STIC and HGSC samples (n = 7) also revealed no statistically significant differences in AR, ER, PI3K, HH, TGF-β and Wnt pathway activity and Ki-67 activity scores (Fig. 1A-G). However, the majority of the STIC samples were characterized by slightly higher AR, ER, PI3K and Wnt pathway activity and lower HH and TGF-β pathway activity as compared to their HGSC counterpart (Fig. S2A-G). For five patients, the samples were taken during interval debulking surgery. In STIC and HGSC samples taken after the start of chemotherapy, we measured higher AR pathway activity and lower HH pathway activity compared to samples taken prior to start of chemotherapy ($P = 0.018$ and P = 0.012, respectively) (Fig. S3A and D). One woman with STIC and concurrent HGSC diagnosis was premenopausal and used a levonorgestrel intrauterine device at the time of surgery. Paired samples of this woman are marked in yellow in Fig. 1A-G and show relatively low AR and high ER pathway activity as compared to the other samples.

3.3. STIC and HGSC samples were characterized by decreased ER and increased PI3K and HH pathway activity in relation to normal FTE samples

Next, we compared the STP activity data from STIC and HGSC samples to STP activity in normal FTE samples. As shown in Fig. 1B-D, we observed significantly lower ER pathway activity as well as higher PI3K and HH pathway activity in both STIC and HGSC samples compared to

Table 1
Summary of clinicopathological characteristics of the included women with normal Fallopian tube epithelium (FTE) and serous tubal intraepithelial carcinoma (STIC) with concurrent high-grade serous carcinoma (HGSC).

	Normal FTE ($n = 8$)	STIC with concurrent HGSC ($n = 8$)	*P*-value*
Age at surgery (years)			0.289
Median (IQR)	62 (59–67)	67 (64–71)	
Menopausal status			1.000
Premenopausal (%)	0 (0)	1 (12)	
Postmenopausal (%)	8 (100)	7 (88)	
BMI (kg/m^2)			0.007
Median (IQR)	27.5 (24.9–29.3)	22.6 (20.6–23.6)	
Parity (number)			1.000
Median (IQR)	2 (2–3)	2 (2–3)	
Missing (n)	2	0	
FIGO disease stage			–
IIIC (%)	–	6 (75)	
IV (%)	–	2 (25)	
Type of treatment			–
Salpingectomy with or without hysterectomy	8 (100)	–	
PDS + ACT	–	3 (37)	
NAC + IDS	–	5 (63)	

Abbreviations: ACT, adjuvant chemotherapy; BMI, body mass index; IDS, Interval debulking surgery; IQR, interquartile range; NAC, Neoadjuvant chemotherapy; PDS, Primary debulking surgery.
* For continuous variables with skewed distribution, P-values were obtained from Wilcoxon rank sum tests. Differences in categorical variables were tested with Fisher's exact tests.

normal FTE samples. For the AR and Wnt pathways, comparable activity was found in normal FTE and STIC samples, while the HGSC samples demonstrated significantly lower AR and Wnt pathway activity as compared to normal FTE samples (Fig. 1A and F). Although TGF-β pathway activity did not differ between the groups, we observed a broad range in activity scores in the HGSC samples (Fig. 1E). Assessment of Ki-67 activity demonstrated significantly higher activity scores in STIC and HGSC samples in comparison to normal FTE samples, indicating increased cell proliferation (Fig. 1G).

3.4. Loss of FOXO3a protein expression in STIC and HGSC samples in comparison to normal FTE samples

We subsequently assessed FOXO3a protein expression by immunohistochemistry in normal FTE, STIC and HGSC samples. Some samples were lost as the areas of interest were no longer present in the consecutive slides. In total, eight normal FTE, six STIC and five HGSC samples were available for FOXO3a protein expression assessment. Representative images of FOXO3a immunohistochemically stained slides are presented in Fig. 2A-C. Interobserver agreement for the FOXO3a histoscore assessment was excellent with an intra-class correlation coefficient based on absolute agreement of 0.916 (95% confidence interval 0.785–0.967). We determined median FOXO3a histoscores of 275 (interquartile range (IQR) 270–286) in normal FTE, 238 (IQR 199–258) in STIC and 215 (IQR 155–220) in HGSC samples. STIC and HGSC samples had significantly lower FOXO3a histoscores in comparison to FTE samples ($P = 0.002$ and $P = 0.033$, respectively) (Fig. 2D). The negative correlation between FOXO3a histoscores and PI3K pathway activity validated the inverse relation between FOXO and PI3K ($P = 0.020$) (Fig. 2E).

4. Discussion

In this study, we assessed the activity of key STPs in normal FTE, STIC and HGSC samples in order to identify early aberrations in STP activity that may drive the development of FTE precursors and progression into HGSC. Among several signaling pathways that await exploration,

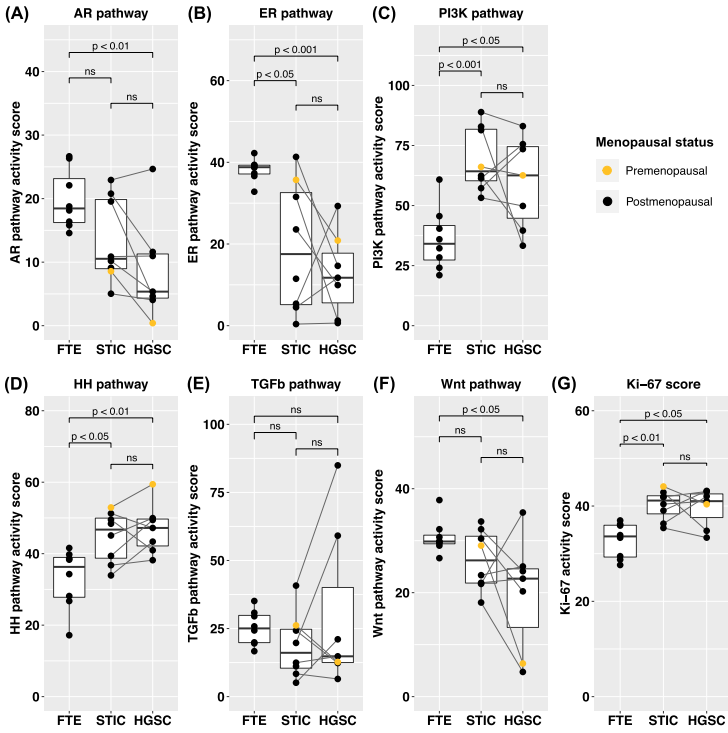

Fig. 1. Boxplots displaying differences in signal transduction pathway activity between Fallopian tube epithelium (FTE) ($n = 8$), serous tubal intraepithelial carcinoma (STIC) (n = 8) and high-grade serous carcinoma (HGSC) samples ($n = 7$). Yellow dots indicate a premenopausal woman with an intrauterine device in situ at the time of surgery. *P*-values were obtained from unpaired Wilcoxon rank sum tests. In addition, paired Wilcoxon signed-rank tests were used to analyze paired STIC and HGSC samples ($n = 7$, indicated with gray lines). A. Androgen receptor (AR). B. Estrogen receptor (ER). C. Phosphoinositide-3-kinase (PI3K). D. Hedgehog (HH). E. Transforming growth factor beta (TGFb). F. Canonical wingless-type MMTV integration site (Wnt). G. Ki-67 activity score. ns = not significant.

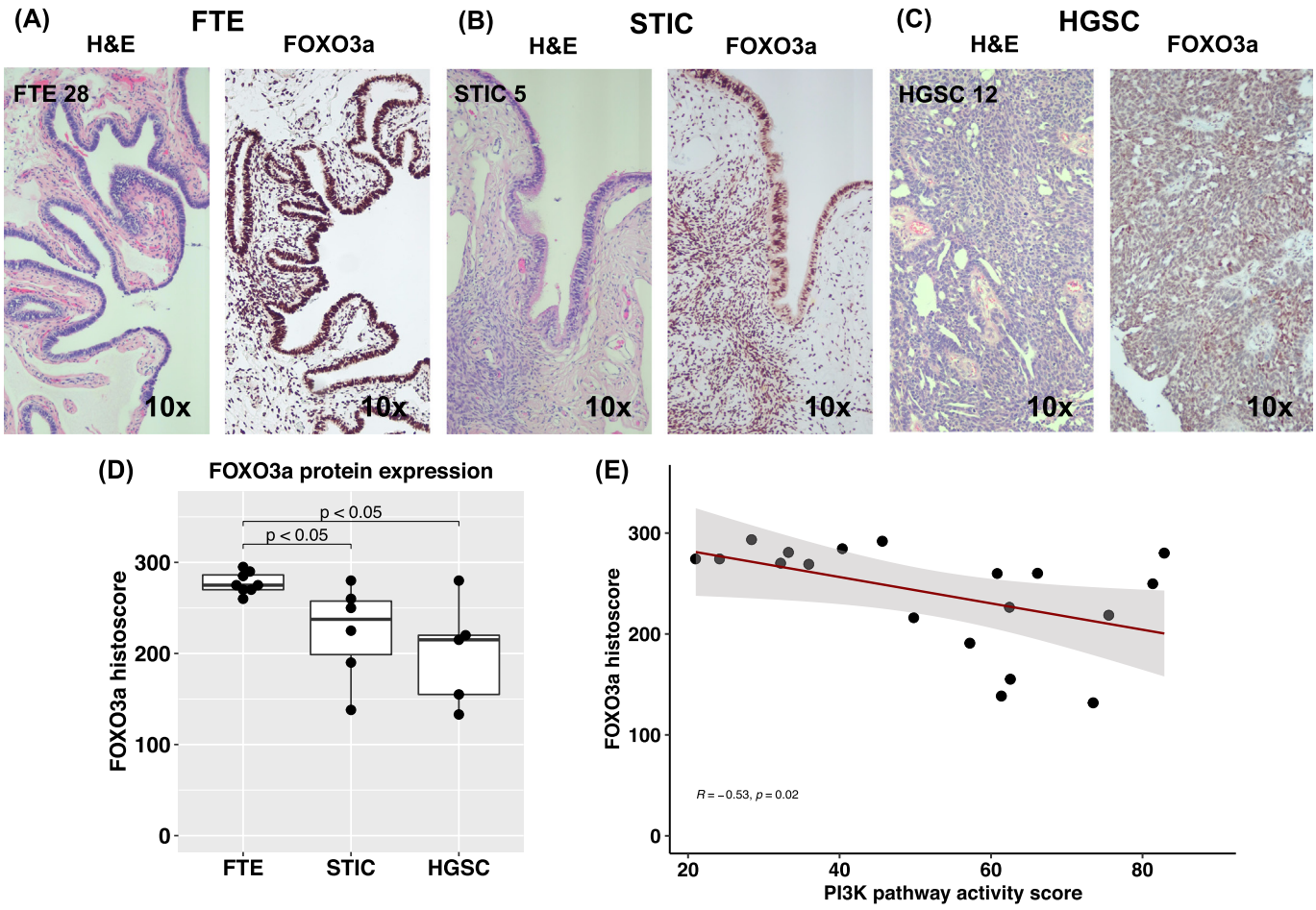

Fig. 2. Forkhead box protein O3a (FOXO3a) protein expression. Representative images of hematoxylin and eosin (H&E) and FOXO3a immunohistochemically stained slides of A. Normal Fallopian tube epithelium (FTE). B. Serous tubal intraepithelial carcinoma (STIC). C. High-grade serous carcinoma (HGSC). D. Boxplots displaying differences in FOXO3a histoscores between the groups (FTE $n = 8$, STIC $n = 6$ and HGSC $n = 5$). P-values were obtained from Wilcoxon rank sum tests. E. FOXO3a histoscores were negatively correlated to phosphoinositide-3-kinase (PI3K) pathway activity scores. The correlation was determined by Spearman's rank correlation coefficient.

we focused on the AR, ER, PI3K, HH, TGF-β and Wnt pathways as these pathways were previously associated to ovarian carcinogenesis [24–29]. Our data provide evidence that loss of ER pathway activity and increased PI3K and HH pathway activity may be underlying events contributing to neoplastic transformation of FTE into STIC, whereas loss of AR and Wnt pathway activity are more likely to be contributors of HGSC progression. With the use of Bayesian models integrating mRNA expression levels of direct pathway-specific target genes, our analysis enabled a unique assessment of the functional pathway activity profile.

We observed comparable Ki-67 activity scores in STIC and concurrent HGSC samples, but significantly higher Ki-67 activity scores compared to normal FTE samples, suggesting a marked increase in proliferative activity in STIC and HGSC samples (Fig. 1G). These observations were in line with previous data on Ki-67 expression by immunohistochemistry in a similar cohort and confirmed that our cohort was representative of STIC and HGSC samples [30]. Overall, we observed similar STP activity across the STIC and HGSC samples, which might also suggest a causal relation with a common biological origin. We were unable to identify any statistically significant relations in STP activity between paired STIC and HGSC samples. However, we noticed subtle patterns in pathway activity up- or downregulation as the majority of the STIC samples had slightly higher AR, ER, PI3K and Wnt pathway activity and lower HH and TGF-β compared to their HGSC counterpart, but small sample sizes may have contributed to lack of statistical significance. Subsequent comparison to normal FTE samples from women who had surgery for benign diagnosis, provided a unique opportunity to assess normal pathway activity and revealed more distinct differences in ER, PI3K and HH pathway activity in STIC and HGSC samples.

Previously, others have implicated a role for PI3K signaling in HGSC development based on loss of FOXO3a protein expression [15,16,31]. Although nuclear FOXO3a protein expression is insufficient to describe functional activity of the PI3K pathway, it provides complementary information and enabled us to compare our results with previously published findings [13]. Levanon et al. investigated the transcriptional profile of normal FTE and HGSC samples and concluded that FOXO3a loss is involved in the pathogenesis of HGSC [13]. In line with results of Levanon et al., we observed significant loss of FOXO3a protein expression in STIC and HGSC samples in comparison to normal FTE samples (Fig. 2D) [13]. The FOXO transcription factor complex is an important downstream component of the PI3K/AKT signaling pathway as phosphorylation by AKT inhibits activity of the FOXO transcription factor and thereby promotes cell proliferation [32]. Thus, in the absence of activated PI3K/AKT, the FOXO transcription factor acts as a tumor suppressor with apoptotic effects. Our data further highlights the significance of PI3K signaling as we found significantly higher PI3K pathway activity in STIC and HGSC samples compared to normal FTE samples (Fig. 1C). Others also found activation of PI3K signaling in STIC based on positive immunohistochemical staining of Stathmin 1 (STMN1), which is considered a surrogate marker for PI3K pathway activity [33,34]. Interestingly, the authors observed negative STMN1 expression in “p53

signatures", known as the morphologically normal putative precursor lesion identified by p53 protein accumulation, but positive STMN1 expression in "proliferative p53 signatures", which are characterized by both p53 and Ki-67 protein expression [33]. The presence of STMN1 expression as early as in these transitional lesions (i.e. proliferative p53 signatures) strongly suggests an association with tumor initiation rather than progression. In addition, mutant p53 in ovarian cancer cells mediated increased phosphorylation of AKT, this suggests an association between p53 and PI3K/AKT signaling [35]. In normal FTE samples from premenopausal woman, our group previously observed a cyclic pattern of PI3K activation during the proliferative phase of the menstrual cycle [36]. Given the tight regulation of PI3K (in)activation in normal FTE, it is likely that aberrations in PI3K signaling disrupt tissue homeostasis and confers a selective advantage to maintain a proliferative state. However, despite the fact that genomic alterations related to the PI3K pathway occur in HGSC, for instance *PIK3CA* amplifications or mutations (2–20%) [37–40], *PTEN* deletions or mutations (7%) [41] and *AKT2* amplifications (18%) [39], these are more frequently found in the endometrioid and clear cell subtypes. These findings, together with our current findings, suggest deregulated FOXO-PI3K signaling as the predominant mechanism during the early stages of serous carcinogenesis rather than genomic changes in the PI3K pathway.

Neoplastic transformation of FTE is likely to require abnormal functioning of several signaling pathways rather than a single pathway, as for instance is the case in the development of colorectal and lung cancer [42]. Besides increased activity of the PI3K pathway, our findings further associated decreased ER pathway activity with STIC and HGSC samples (Fig. 1B). Although the association between estrogen replacement therapy and ovarian cancer risk and the frequent expression of the ER protein suggest hormone sensitivity, the function of estrogen signaling in terms of tumor initiation and progression is still not understood [43]. On the contrary, the use of anti-estrogen therapy has been associated with tubal dysplasia [44]. Our results show that normal ER pathway activity, which is necessary to preserve normal function of the Fallopian tube, is obviously decreased in STIC samples and even lost in HGSC samples (Fig. 1B). It must be noted that the difference in ER pathway activity may be influenced by the amount of estrogen producing adipose tissue as women in the normal FTE group had a higher BMI when compared to women in the STIC and HGSC group ($P = 0.007$). Further validation on the exact role of ER signaling is needed to identify whether loss of ER pathway activity in particular triggers cellular differentiation and proliferation or, alternatively, is caused by the tumor-driving effects of other signaling pathways, such as aberrant PI3K signaling. Nevertheless, loss of functional activity of the ER pathway would at least explain the limited response to anti-estrogen receptor targeted drugs in patients diagnosed with HGSC [45].

Another finding of our analysis is hyperactivation of the HH pathway with limited variation between paired STIC and HGSC samples (Fig. 1D). Given the tumor-promoting role of HH signaling in a wide variety of cancers, including ovarian carcinoma, the involvement of HH pathway activity in STIC is not surprising [46,47]. Previous studies revealed a collaboration between p53 and HH signaling and found that p53 negatively regulated GLI1 expression, a downstream effector of HH signaling [48,49]. Thereby, the high incidence of *TP53* mutations in STIC and HGSC could explain the increase in HH activity by loss of the inhibitory effect of p53 signaling on GLI1. Moreover, in ovarian cancer cells, an interplay between the PI3K and HH pathway has been described as PI3K/AKT signaling was found to enhance GLI1 activity, a downstream effector of HH signaling [50,51]. The induced activity of PI3K and HH signaling upon progression to STIC and HGSC suggests synergistic activation. However, the exact role of PI3K and HH crosstalk in STIC is currently unknown and requires future work. To further support the causality between aberrant pathway activity and early serous carcinogenesis, future studies might benefit from ex vivo oviduct cultures or organoids, which allow experimental conditions to investigate the effect of pathway activators and inhibitors.

Our study was limited by small sample size and technical challenges to acquire sufficient epithelial cells of small areas with STIC in consecutive slides. Unfortunately, we had to exclude some samples due to low input amounts and lost samples in the analysis of FOXO3a protein expression. Moreover, cytotoxic treatment affects STP activity and therefore has influenced the STP results in samples taken after the start of chemotherapy. In addition, it should be considered that some STIC may have represented metastases of HGSC onto the tubal epithelium and mimic de novo STIC, as described previously [11]. To rule out these confounding factors and further investigate the role of STP activity in serous carcinogenesis, a prospective study should be performed focusing on the presence of "p53 signatures" and incidental STIC in the Fallopian tubes of patients with benign diagnosis.

A major strength of the study is the quantification of STP activity from transcription factor-specific target gene mRNA levels enabling functional activity scores. More importantly, as we determined the activity of key signaling pathways with clinical target in normal tissue, the pathway-specific range may be used as benchmark to define aberrant activity in individual HGSC samples. Therefore, once the range of normal STP activity has been validated on a larger set of samples, this approach could help guide the selection of patients for targeted therapy based on abnormal STP activity.

Taken together, our findings implicate a distinct role for hyperactivation of the PI3K signaling pathway as a putative early driver in the neoplastic transformation of FTE. Moreover, we show low ER and high HH signaling pathway activity in STIC and concurrent HGSC samples compared to FTE samples, suggesting these STPs are associated with the transition to neoplasia, whereas advanced disease is further characterized by loss of AR and Wnt pathway activity. Although much remains to be discovered on the exact role of these pathways during the early events of HGSC initiation and progression, our results open new perspectives on the molecular processes contributing to the pathogenesis of HGSC.

Supplementary data to this article can be found online at https://doi.org/10.1016/j.ygyno.2022.01.027.

Funding

This study was supported in part by Molecular Pathway Diagnostics, Philips.

Author's contribution

PvdP and JMJP designed the study; PvdP and AU collected the data and performed the experiments; SLB and PJvD performed the pathological assessments; YJWWR and AvdS contributed to pathway activity analysis; PvdP wrote the initial manuscript; SL, RLMB, JMJP contributed to data interpretation and supervised the project. All authors revised the manuscript for important intellectual content and approved the final version to be published.

Declaration of Competing Interest

PvdP is employed by the Catharina Hospital, where her research is funded by the Catharina Research fund and Molecular Pathway Diagnostics, Philips. YJWWR and AvdS are employed by Molecular Pathway Diagnostics, Philips. The other authors declare no competing interests.

Acknowledgments

We gratefully acknowledge the laboratory staff of Stichting PAMM for their technical assistance, Erica Sierra-de Koning for her support with laser capture microdissection and Domenico Castigliego and Sevda Karakus for their contribution to FOXO3a immunohistochemistry. Furthermore, the authors would like to thank Eveline den Biezen-Timmermans, Diederick Keizer, Sieglinde Neerken, Dianne van Strijp,

Saskia Vermeer-van de Laar, Paul van de Wiel for their valuable assistance in data analysis.

References

[1] J.S. Berek, S.T. Kehoe, L. Kumar, M. Friedlander, Cancer of the ovary, fallopian tube, and peritoneum, Int. J. Gynaecol. Obstet. 143 (Suppl. 2) (2018) 59–78.
[2] H. Karagol, P. Saip, Y. Eralp, S. Topuz, S. Berkman, R. Ilhan, et al., Factors related to recurrence after pathological complete response to postoperative chemotherapy in patients with epithelial ovarian cancer, Tumori. 95 (2009) 207–211.
[3] V. Ghirardi, M.C. Moruzzi, N. Bizzarri, V. Vargiu, M. D'Indinosante, G. Garganese, et al., Minimal residual disease at primary debulking surgery versus complete tumor resection at interval debulking surgery in advanced epithelial ovarian cancer: A survival analysis, Gynecol. Oncol. 157 (2020) 209–213.
[4] J. Kim, E.Y. Park, O. Kim, J.M. Schilder, D.M. Coffey, C.H. Cho, et al., Cell origins of high-grade serous ovarian Cancer, Cancers (Basel). 10 (2018).
[5] J.M. Piek, P.J. van Diest, R.P. Zweemer, J.W. Jansen, R.J. Poort-Keesom, F.H. Menko, et al., Dysplastic changes in prophylactically removed fallopian tubes of women predisposed to developing ovarian cancer, J. Pathol. 195 (2001) 451–456.
[6] J.M. Piek, R.H. Verheijen, F.H. Menko, A.P. Jongsma, J. Weegenaar, J.J. Gille, et al., Expression of differentiation and proliferation related proteins in epithelium of prophylactically removed ovaries from women with a hereditary female adnexal cancer predisposition, Histopathology. 43 (2003) 26–32.
[7] D.W. Kindelberger, Y. Lee, A. Miron, M.S. Hirsch, C. Feltmate, F. Medeiros, et al., Intraepithelial carcinoma of the fimbria and pelvic serous carcinoma: evidence for a causal relationship, Am. J. Surg. Pathol. 31 (2007) 161–169.
[8] E. Kuhn, R.J. Kurman, R. Vang, A.S. Sehdev, G. Han, R. Soslow, et al., TP53 mutations in serous tubal intraepithelial carcinoma and concurrent pelvic high-grade serous carcinoma–evidence supporting the clonal relationship of the two lesions, J. Pathol. 226 (2012) 421–426.
[9] R. Perets, G.A. Wyant, K.W. Muto, J.G. Bijron, B.B. Poole, K.T. Chin, et al., Transformation of the fallopian tube secretory epithelium leads to high-grade serous ovarian cancer in Brca;Tp53;Pten models, Cancer Cell 24 (2013) 751–765.
[10] Y. Yamamoto, G. Ning, B.E. Howitt, K. Mehra, L. Wu, X. Wang, et al., In vitro and in vivo correlates of physiological and neoplastic human fallopian tube stem cells, J. Pathol. 238 (2016) 519–530.
[11] M.A. Eckert, S. Pan, K.M. Hernandez, R.M. Loth, J. Andrade, S.L. Volchenboum, et al., Genomics of ovarian Cancer progression reveals diverse metastatic trajectories including intraepithelial metastasis to the fallopian tube, Cancer Discov. 6 (2016) 1342–1351.
[12] J. Ducie, F. Dao, M. Considine, N. Olvera, P.A. Shaw, R.J. Kurman, et al., Molecular analysis of high-grade serous ovarian carcinoma with and without associated serous tubal intra-epithelial carcinoma, Nat. Commun. 8 (2017) 990.
[13] K. Levanon, S. Sapoznik, K. Bahar-Shany, H. Brand, R. Shapira-Frommer, J. Korach, et al., FOXO3a loss is a frequent early event in high-grade pelvic serous carcinogenesis, Oncogene. 33 (2014) 4424–4432.
[14] M. Hornsveld, T.B. Dansen, P.W. Derksen, B.M.T. Burgering, Re-evaluating the role of FOXOs in cancer, Semin. Cancer Biol. 50 (2018) 90–100.
[15] M. Lu, Y. Zhao, F. Xu, Y. Wang, J. Xiang, D. Chen, The expression and prognosis of FOXO3a and Skp2 in human ovarian cancer, Med. Oncol. 29 (2012) 3409–3415.
[16] M. Fei, Y. Zhao, Y. Wang, M. Lu, C. Cheng, X. Huang, et al., Low expression of Foxo3a is associated with poor prognosis in ovarian cancer patients, Cancer Investig. 27 (2009) 52–59.
[17] L. van Lieshout, A. van de Stolpe, P. van der Ploeg, D. Bowtell, J. de Hullu, J. Piek, Signal transduction pathway activity in high-grade, serous ovarian carcinoma reveals a more favorable prognosis in tumors with low PI3K and high NF-kappaB pathway activity: A novel approach to a long-standing enigma, Cancers (Basel). 12 (2020).
[18] H. van Ooijen, M. Hornsveld, C. Dam-de Veen, R. Velter, M. Dou, W. Verhaegh, et al., Assessment of functional phosphatidylinositol 3-kinase pathway activity in cancer tissue using Forkhead box-O target gene expression in a knowledge-based computational model, Am. J. Pathol. 188 (2018) 1956–1972.
[19] W. Verhaegh, H. van Ooijen, M.A. Inda, P. Hatzis, R. Versteeg, M. Smid, et al., Selection of personalized patient therapy through the use of knowledge-based computational models that identify tumor-driving signal transduction pathways, Cancer Res. 74 (2014) 2936–2945.
[20] A. van de Stolpe, W. Verhaegh, J.Y. Blay, C.X. Ma, P. Pauwels, M. Pegram, et al., RNA based approaches to profile oncogenic pathways from low quantity samples to drive precision oncology strategies, Front. Genet. 11 (2020), 598118.
[21] A. van de Stolpe, L. Holtzer, H. van Ooijen, M.A. Inda, W. Verhaegh, Enabling precision medicine by unravelling disease pathophysiology: quantifying signal transduction pathway activity across cell and tissue types, Sci. Rep. 9 (2019) 1603.
[22] A. van de Stolpe, Quantitative measurement of functional activity of the PI3K signaling pathway in Cancer, Cancers (Basel). 11 (2019).
[23] W.J. van Weelden, L.J.M. van der Putten, M.A. Inda, A. van Brussel, M. Snijders, L.M.M. Schriever, et al., Oestrogen receptor pathway activity is associated with outcome in endometrial cancer, Br. J. Cancer 123 (2020) 785–792.
[24] T. Mizushima, H. Miyamoto, The role of androgen receptor signaling in ovarian cancer, Cells. 8 (2019).
[25] S.P. Langdon, C.S. Herrington, R.L. Hollis, C. Gourley, Estrogen signaling and its potential as a target for therapy in ovarian cancer, Cancers (Basel). 12 (2020).
[26] M.K. Ediriweera, K.H. Tennekoon, S.R. Samarakoon, Role of the PI3K/AKT/mTOR signaling pathway in ovarian cancer: biological and therapeutic significance, Semin. Cancer Biol. 59 (2019) 147–160.
[27] J. Szkandera, T. Kiesslich, J. Haybaeck, A. Gerger, M. Pichler, Hedgehog signaling pathway in ovarian cancer, Int. J. Mol. Sci. 14 (2013) 1179–1196.
[28] B.M. Roane, R.C. Arend, M.J. Birrer, Review: targeting the transforming growth factor-beta pathway in ovarian cancer, Cancers (Basel) 11 (2019).
[29] M. Teeuwssen, R. Fodde, Wnt signaling in ovarian cancer stemness, EMT, and therapy resistance, J. Clin. Med. 8 (2019).
[30] E. Kuhn, R.J. Kurman, A.S. Sehdev, Ie M. Shih, Ki-67 labeling index as an adjunct in the diagnosis of serous tubal intraepithelial carcinoma, Int. J. Gynecol. Pathol. 31 (2012) 416–422.
[31] J. Zhang, J.C. Wang, Y.H. Li, R.X. Wang, X.M. Fan, Expression of PH domain leucine-rich repeat protein phosphatase, Forkhead Homeobox type O 3a and RAD51, and their relationships with Clinicopathologic features and prognosis in ovarian serous adenocarcinoma, Chin. Med. J. 130 (2017) 280–287.
[32] A. Brunet, A. Bonni, M.J. Zigmond, M.Z. Lin, P. Juo, L.S. Hu, et al., Akt promotes cell survival by phosphorylating and inhibiting a Forkhead transcription factor, Cell. 96 (1999) 857–868.
[33] A.M. Karst, K. Levanon, S. Duraisamy, J.F. Liu, M.S. Hirsch, J.L. Hecht, et al., Stathmin 1, a marker of PI3K pathway activation and regulator of microtubule dynamics, is expressed in early pelvic serous carcinomas, Gynecol. Oncol. 123 (2011) 5–12.
[34] M. Novak, J. Lester, A.M. Karst, V. Parkash, M.S. Hirsch, C.P. Crum, et al., Stathmin 1 and p16(INK4A) are sensitive adjunct biomarkers for serous tubal intraepithelial carcinoma, Gynecol. Oncol. 139 (2015) 104–111.
[35] J.G. Lee, J.H. Ahn, T. Jin Kim, J. Ho Lee, J.H. Choi, Mutant p53 promotes ovarian cancer cell adhesion to mesothelial cells via integrin beta4 and Akt signals, Sci. Rep. 5 (2015) 12642.
[36] P. van der Ploeg, A. Uittenboogaard, K.M.M. Bucks, M.H.F.M. Lentjes-Beer, S.L. Bosch, M.M.E. van Rumste, et al., Cyclic activity of signal transduction pathways in fimbrial epithelium of the human fallopian tube, Acta Obstet Gynecol Scand. (2021) In press.
[37] I.G. Campbell, S.E. Russell, D.Y. Choong, K.G. Montgomery, M.L. Ciavarella, C.S. Hooi, et al., Mutation of the PIK3CA gene in ovarian and breast cancer, Cancer Res. 64 (2004) 7678–7681.
[38] U.A. Matulonis, M. Hirsch, E. Palescandolo, E. Kim, J. Liu, P. van Hummelen, et al., High throughput interrogation of somatic mutations in high grade serous cancer of the ovary, PLoS One 6 (2011), e24433.
[39] K. Nakayama, N. Nakayama, R.J. Kurman, L. Cope, G. Pohl, Y. Samuels, et al., Sequence mutations and amplification of PIK3CA and AKT2 genes in purified ovarian serous neoplasms, Cancer Biol. Ther. 5 (2006) 779–785.
[40] B. Cheaib, A. Auguste, A. Leary, The PI3K/Akt/mTOR pathway in ovarian cancer: therapeutic opportunities and challenges, Chin. J. Cancer. 34 (2015) 4–16.
[41] Cancer Genome Atlas Research N, Integrated genomic analyses of ovarian carcinoma, Nature. 474 (2011) 609–615.
[42] C. Tomasetti, L. Marchionni, M.A. Nowak, G. Parmigiani, B. Vogelstein, Only three driver gene mutations are required for the development of lung and colorectal cancers, Proc. Natl. Acad. Sci. U. S. A. 112 (2015) 118–123.
[43] V. Beral, K. Gaitskell, C. Hermon, K. Moser, G. Reeves, et al., Collaborative Group on Epidemiological Studies of Ovarian C, Menopausal hormone use and ovarian cancer risk: individual participant meta-analysis of 52 epidemiological studies, Lancet 385 (2015) 1835–1842.
[44] G. Chene, N. Radosevic-Robin, A.S. Tardieu, A. Cayre, I. Raoelfils, P. Dechelotte, et al., Morphological and immunohistochemical study of ovarian and tubal dysplasia associated with tamoxifen, Eur. J. Histochem. 58 (2014) 2251.
[45] P. van der Ploeg, M. Ottenheijm, L. van Lieshout, A. van de Stolpe, S. Bosch, A. Thijs, et al., Efficacy of anti-hormonal therapy in estrogen receptor positive high-grade serous ovarian carcinoma: a systematic review, J. Cancer Sci. Clin. Therap. 4 (2020) 237–257.
[46] L. Yang, G. Xie, Q. Fan, J. Xie, Activation of the hedgehog-signaling pathway in human cancer and the clinical implications, Oncogene. 29 (2010) 469–481.
[47] R. Bhattacharya, J. Kwon, B. Ali, E. Wang, S. Patra, V. Shridhar, et al., Role of hedgehog signaling in ovarian cancer, Clin. Cancer Res. 14 (2008) 7659–7666.
[48] Y. Abe, E. Oda-Sato, K. Tobiume, K. Kawauchi, Y. Taya, K. Okamoto, et al., Hedgehog signaling overrides p53-mediated tumor suppression by activating Mdm2, Proc. Natl. Acad. Sci. U. S. A. 105 (2008) 4838–4843.
[49] B. Stecca, Ruiz i Altaba A., A GLI1-p53 inhibitory loop controls neural stem cell and tumour cell numbers, EMBO J. 28 (2009) 663–676.
[50] R. Singh, P.K. Dhanyamraju, M. Lauth, DYRK1B blocks canonical and promotes non-canonical hedgehog signaling through activation of the mTOR/AKT pathway, Oncotarget. 8 (2017) 833–845.
[51] Z. Ke, S. Caiping, Z. Qing, W. Xiaojing, Sonic hedgehog-Gli1 signals promote epithelial-mesenchymal transition in ovarian cancer by mediating PI3K/AKT pathway, Med. Oncol. 32 (2015) 368.